
We present a systematic study of the properties of sintered silver powders used in heat exchangers at millikelvin temperatures. Scanning electron microscopy and surface area (BET) measurements have been performed on various powders with different degrees of sintering. Values of the Kapitza resistance with pure He³ and He³-He⁴ mixtures are given and compared with previously reported results.

Properties of sintered silver powders and their application in heat exchangers at millikelvin temperatures

H. Franco, J. Bossy and H. Godfrin

Key words: cryogenics, sintered silver, heat exchanger

Sintered metallic powders are commonly used in low temperature research to increase the boundary surface area between a solid and liquid or solid helium.¹

Wheatley and coworkers⁴ first used sintered copper powders to enhance the heat transfer in the exchangers of a dilution refrigerator. Sintered silver powders are presently more popular, after the work of Radebaugh, Siegwarth and Holste⁵ and Frossati and Thoulouze.⁶ Steady state temperatures as low as 2 mK are reached in our laboratory by using sintered silver heat exchangers with a total surface area of the order of 200 m².⁷ These applications are one aspect of the understanding of the mechanisms of the heat transfer which are of fundamental importance.^{2,3,8,9} A characterization of the sintered powders is therefore desirable. Krusius, Paulson and Wheatley¹⁰ published the first study of copper sintered powders. Most recently, Robertson, Guillon and Harrison¹¹ have measured various properties of sintered copper and silver powders and described them in the framework of a simple model.

We describe in this article a systematic study of the properties of the silver powders used in the construction of heat exchangers, and their evolution during the sintering procedure.

Sample preparation

Silver powders. Three types of silver powders have been studied:

- 'French powder': grain size $\lesssim 1 \mu\text{m}$.¹²
- '700Å Japanese powder': grain size $\sim 70 \text{ nm}$.¹³
- '400Å Japanese powder': grain size $\sim 40 \text{ nm}$.¹³

Sintering procedure. The powder was placed in a rectangular mould, dimensions 3.4 cm \times 1.9 cm, and pressed at 460 kg cm⁻². The final thickness was $\sim 0.7 \text{ mm}$, and the density $\sim 45\%$ of that of bulk silver. The resulting sponge was self sustaining, although fra-

gile, for the Japanese powders,⁷ but not for the French one, at least at the pressure we have used.

The sponge was then introduced in a stainless steel container, which was pumped (vacuum $\lesssim 10^{-2}$ mbar), and then filled with a mixture of 90% argon + 10% hydrogen at an absolute pressure of 0.75 bar. The container was introduced in an oven preheated to the desired temperature ($\sim 200^\circ\text{C}$).

The temperature was measured by a thermocouple located close to the sample. About 40 min were needed to reach the final temperature, which was maintained for 45 min. The container was then removed, and allowed to cool down at room temperature in about 40 min.

Note that no pressure (ie no jigs or plastic pistons⁷) was applied to the sponge during the sintering process.

We use the following codes to define the samples
French powder. FO: powder as taken from the bottle, F(160): sintered at 160°C.

700Å Japanese powder. J70: powder as taken from the bottle, J7C: compressed powder, J7(T): five samples, sintered at the temperature T (degrees Celsius): J7(160), J7(190), J7(200), J7(265); J7A0: powder as taken from a different bottle and J7A(160): powder J7A0 sintered at 160°C.

400Å Japanese powder. J40: powder as taken from the bottle, J4(250): sintered at $T \sim 250^\circ\text{C}$ (the sintering conditions were not controlled as precisely as for the other samples).

Scanning electron microscope (SEM) measurements

The pictures shown in this section have been obtained with a scanning electron microscope.

The scale (a white line at the lower right corner), its length (for example: 1.0U is 1.0 μm), and the magnification (for example $\times 60000$), are indicated on each picture.

The sintered samples were broken to observe the structure inside the sinter.

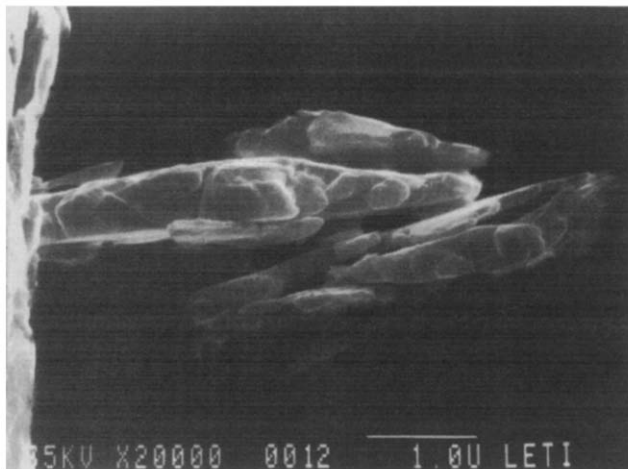


Fig. 1 French powder; the scale (1 μm) is given by the white line at the lower right corner of the picture

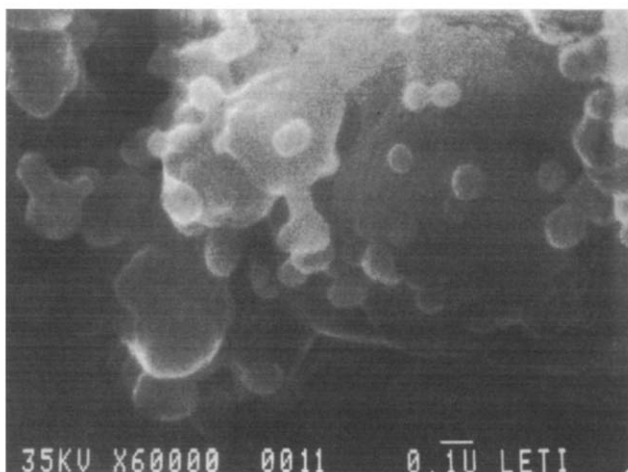


Fig. 2 Japanese 700Å powder; scale (0.1 μm) given by the white line

French powder

Samples FO and F(160): The shape of the particles is shown in Fig. 1, the flakes are quite asymmetrical, and the size scale is of the order of 1 μm . They have a tendency to pile up like plates, and this explains the difficulty of obtaining a self sustaining sponge by compression of this powder. The same orientational effect is found in the sinter, sample F (160).

700 Å Japanese powder

Stage 1: The powder as taken from the bottle (sample J70). The 700 Å Japanese powder has a quite different shape, as can be seen on Fig. 2. The particles are rather spherical; their size is of the order of 0.1 μm . Large clusters (diameter \sim 0.5 μm) of particles are also seen, with a structure at the size scale of the individual particles; it is difficult to decide whether the particles are sintered or simply form an aggregate.

Stage 2: The powder after compression, sample J7C. The SEM pictures show only large clusters \sim 0.5 μm .

Stage 3: The sinter after heat treatment at a temperature given for each sample:

Sample J7(160): Only large clusters are seen, Fig. 3. Their size (\sim 0.4 μm) is somewhat smaller than the one measured in the compressed sample, J7C.

Sample J7(190): Important qualitative changes show up at this temperature (190°C). The clusters appear to be much smaller than at previous stages of heat treatment; Fig. 4 shows up much thinner structure than Fig. 3. The size scale is now of the order of 0.1 μm , ie, the particles of the original powder appear individually. This can be clearly seen on Fig. 5; large clusters (\sim 0.3 μm) coexist with particles (\sim 0.1 μm) slightly sintered, which form 'chains' or 'rings'. This effect will be discussed further on.



Fig. 3 Japanese 700Å powder sintered at 160°C: Sample J7(160). Scale (1 μm) given by the white line

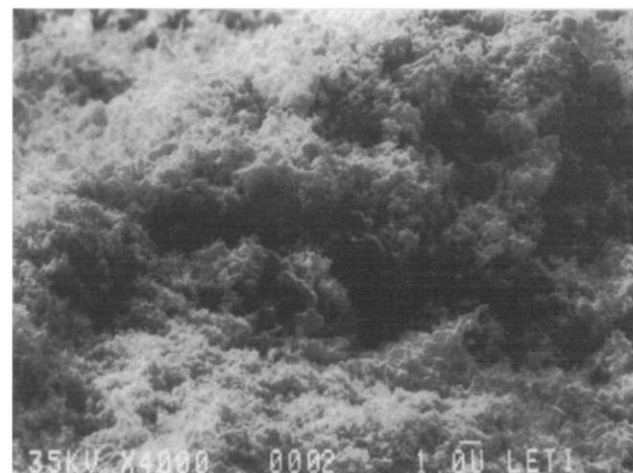


Fig. 4 Japanese 700 Å powder sintered at 190°C: Sample J7(190). Same scale as Fig. 3. Note the decrease in particle size as the heat treatment temperature increases

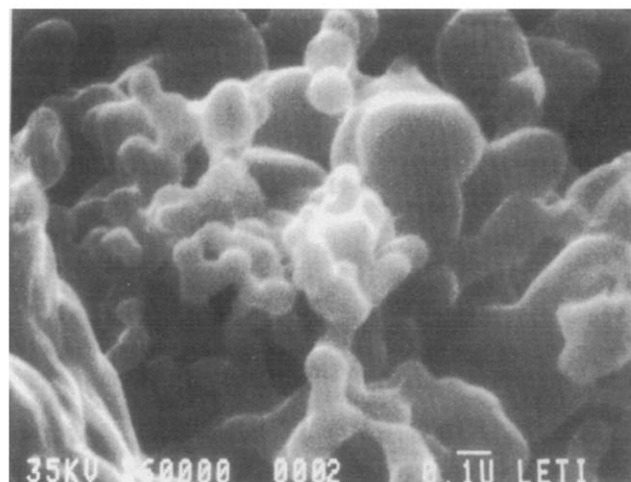


Fig. 5 Enlarged view of Fig. 4. Scale (0.1 μm) given by the white line

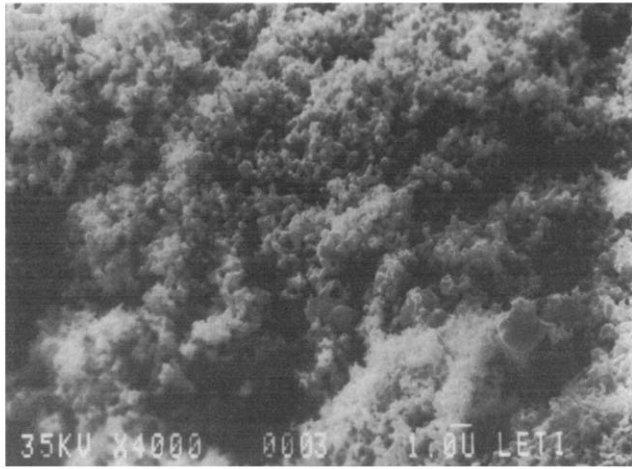


Fig. 6 Japanese 700Å powder sintered at 200°C: Sample J7(200). Same scale as Fig. 3. The particle size increases now with the heat treatment temperature

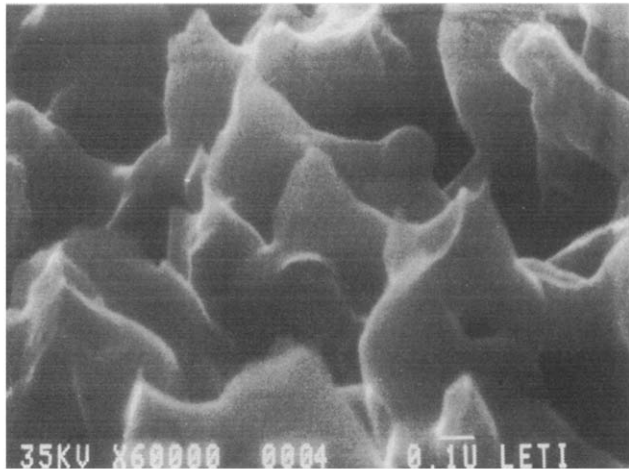


Fig. 7 Japanese 700Å powder sintered at 230°C: Sample J7(230). Scale (0.1 μm) given by the white line. A comparison with Fig. 5 clearly demonstrates the particles growth

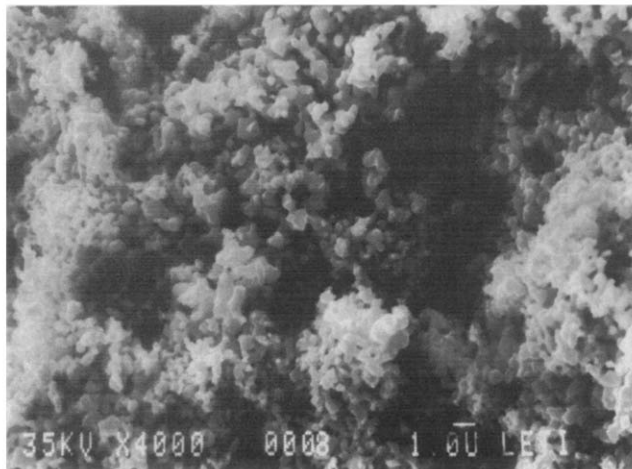


Fig. 8 Japanese 700Å powder sintered at 265°C: Sample J7(265). Same scale as Fig. 3. Figs 3, 4, 6 and 8 show the evolution of the particle size with the sintering temperature

Sample J7(200): At 200°C only small regions of the sample show structures with dimensions $\sim 0.1 \mu\text{m}$. The sinter looks rather homogeneous, with particles $\sim 0.3 \mu\text{m}$, Fig. 6.

Sample J7(230): The particles have grown, reaching a size $\sim 0.4 \mu\text{m}$, Fig. 7. Sharp points can be

observed on the surface along which the sinter was broken; sintering at this temperature produces a mechanically resistant material.

Sample J7(265): The particles are even larger, $\sim 0.5 \mu\text{m}$, and more regular in size. A comparison of Figs 4 and 8 shows clearly the evolution of the grain size with the heat treatment.

We have also studied samples J7A0, J7A(160), taken from another bottle of the same type of powder (nominal 700Å). The grain size was found to be roughly twice as large as that of the former sample. This was also expected from the observation of the colour of the powder (usually dark grey, the particle size being smaller than the light's wavelength) which was definitely lighter than that of sample J70.

Conclusions on the SEM measurements. We conclude that the size of the particles of the Japanese powder is of the order of $0.1 \mu\text{m}$, even if larger clusters are seen, which are certainly loosely bound. These clusters are not individual particles, as suggested in earlier works¹¹ made with a smaller resolution of the SEM.

A compression of the powder favours the growth of the clusters to sizes $\sim 0.5 \mu\text{m}$. But a moderate heat treatment produces a material with a smaller size scale, $\sim 0.1 \mu\text{m}$. Higher temperatures ($\geq 200^\circ\text{C}$) are needed to observe an effective sintering accompanied by a substantial growth of the particles and an important enhancement of the mechanical resistance of the sample.

It seems reasonable to attribute this behaviour to a contamination of the powder. A heat treatment of a large amount of powder, $\sim 1 \text{ kg}$, in a quartz tube under high vacuum, flushed with hydrogen, results in degassing at $T \sim 150^\circ\text{C}$, of a substance which looks like wax and condenses on the cold walls of the tube.¹⁸ Its weight fraction is of the order of 0.5%.

It is not surprising therefore to see clusters of particles in the samples which have been treated at temperatures below $\sim 200^\circ\text{C}$, including the original powder. This also explains the growth of the clusters with the compression of the powder, and the reduction of the cluster size with the heat treatment.

Above 200°C , sintering occurs very efficiently, and the particle size grows.

The processes of degassing and sintering are in competition to determine the 'effective size' of the powder, since their characteristic temperatures are practically equal.

400Å Japanese powder

Sample J40: The powder, as taken from the bottle, is very similar to the 700Å one. The particles are rather spherical, with a size $\sim 0.05 \mu\text{m}$. Clusters are also seen, but their size, $\sim 0.15 \mu\text{m}$, is relatively small.

Sample J4(250): After sintering at $\sim 250^\circ\text{C}$, the size scale of the particles, uniform in all the sample, is of the order of $0.1 \mu\text{m}$. Sharp points can be observed on the surface along which the sinter was broken; sintering at this temperature produces a mechanically resistant material.

The experimental observations and therefore the conclusions are similar to those concerning the 700Å powder. The powder contains clusters due a contamination of the surface. Heat treatment results in

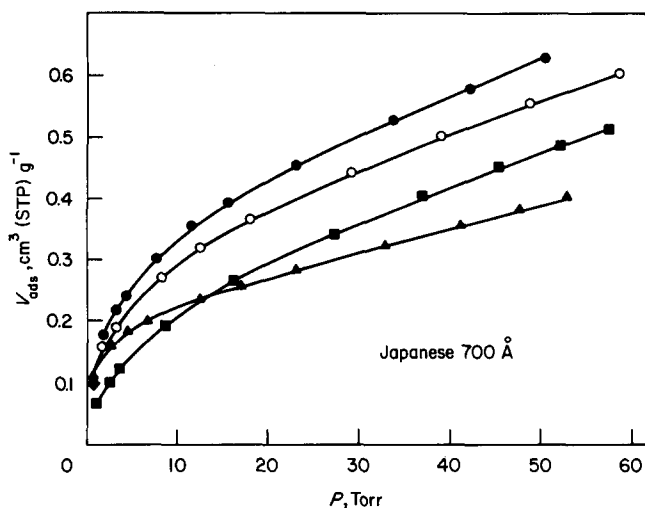


Fig. 9 Argon adsorption isotherms at 77 K on Japanese 700 Å silver powder: Volume (STP) of adsorbed argon gas per gram of silver as a function of the equilibrium pressure. ● powder; ○ compressed powder; ■ sintered at 160°C; △ sintered at 265°C

degassing and sintering of the powder in the same conditions.

Surface area (BET) measurements

The surface area of the sintered silver samples was measured by standard BET adsorption isotherm techniques.^{14,15}

The samples were located in a cell, and degassed by pumping with a liquid nitrogen trapped diffusion pump during 3 h. The temperature of the cell was raised up to 60°C during 30 min during degassing. These conditions correspond to standard operation of the sintered material.

The cell was then cooled down to 77 K, a suitable temperature for argon adsorption isotherms.¹⁷

The amounts of argon gas were measured at room temperature with a calibrated volume and a Baratron MKS 77 pressure gauge. The latter was also used to determine the equilibrium pressures of the adsorption isotherm, in the range 1–60 torr.

The results are presented, as usual, as plots of the adsorbed quantity of argon, expressed in cm³ of gas (STP) per gram of adsorbent, as a function of pressure, Fig. 9.

These curves can be described by the BET equations and were fitted to the linear form¹⁵

$$\frac{x}{v(1-x)} = \frac{1}{v_m C} + \frac{C-1}{v_m C} x$$

where v is the volume of gas adsorbed at a pressure P , v_m the STP volume of gas necessary to form a complete monolayer; x is P/P_0 , where P_0 is the saturation pressure of the vapour (~ 188 torr). The parameter C is related to the heat of adsorption.¹⁵

Both v_m and C are obtained by fitting $x/v(1-x)$ as a function of x by a straight line. The fit is excellent for $0.05 < x < 0.35$.

The results are summarized in the following table; specific surface areas S are obtained from the measured v_m by assuming a coverage of 13.8 \AA^2 per atom, that is 0.27 cm^3 of gas per m^2 of adsorbent,¹⁶ which is practically equal to the value reported by Daunt and Lerner,¹⁷ $0.29 \text{ cm}^3 \text{ m}^{-2}$. The mass of the samples was $\sim 2 \text{ g}$ and the packing fraction $\sim 45\%$.

Discussion of the BET results (Table 1)

Japanese 700 Å powder. As already seen by microscopy techniques, Japanese powders from two batches of the same type '700 Å' (samples J70 and J7A0) do not have the same particle size. The specific surface areas differ by almost a factor 2. The absolute values, $1.88 \text{ m}^2 \text{ g}^{-1}$ and $1.09 \text{ m}^2 \text{ g}^{-1}$ are of the order of that measured by Robertson et al¹¹ ie $1.14 \text{ m}^2 \text{ g}^{-1}$. This surface area is low compared with what is expected for $\sim 0.1 \text{ }\mu\text{m}$ particles ie $\geq 6 \text{ m}^2 \text{ g}^{-1}$. After compression only $\sim 10\%$ of the surface area is lost. With a heat treatment at 160°C, 18% of the surface is lost and the C coefficient decreases by a factor of 2.

For a sintering temperature $T_s = 200^\circ\text{C}$, the surface area, $1.69 \text{ m}^2 \text{ g}^{-1}$, is larger than that at 160 °C; for $T_s \geq 200^\circ\text{C}$, the measured surface area decreases rapidly with T_s , and is only $1.17 \text{ m}^2 \text{ g}^{-1}$ for $T_s = 265^\circ\text{C}$, Fig. 10.

C , the free energy of adsorption, increases with the heat treatment above 200°C , Fig. 11. This can also be seen in Fig. 9, the isotherm at $T = 265^\circ\text{C}$ crosses the other curves showing that a substantial adsorption occurs even at low pressures.

The measured surface area, $\sim 1 \text{ m}^2 \text{ g}^{-1}$, for the

Table 1. Properties of sintered silver powders

	Sample	$v_m, \text{cm}^3 \text{ (STP) g}^{-1}$	$s, \text{m}^2 \text{ g}^{-1}$	C_{BET}
French powder Sintered	FO	0.35	1.3	13
	F(160)	0.18	0.66	6
Japanese 700 Å Compressed Sintered Sintered Sintered Sintered	J70	0.508	1.88	29
	J7C	0.453	1.67	25.5
	J7(160)	0.416	1.54	14
	J7(200)	0.456	1.69	14
	J7(230)	0.386	1.42	21
	J7(265)	0.317	1.17	25
Japanese powder 700 Å (other bottle)	J7A0	0.295	1.09	24
Japanese powder 400 Å	J40	0.691	2.56	37

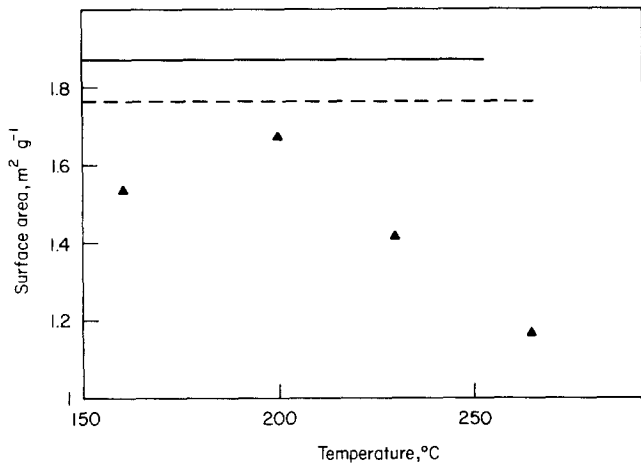


Fig. 10 Surface area of Japanese 700Å sintered powders as a function of the heat treatment temperature. The solid line indicates the surface area of the powder, and the broken line that of the compressed powder. Note the larger value of the surface area for $T \sim 200^\circ\text{C}$

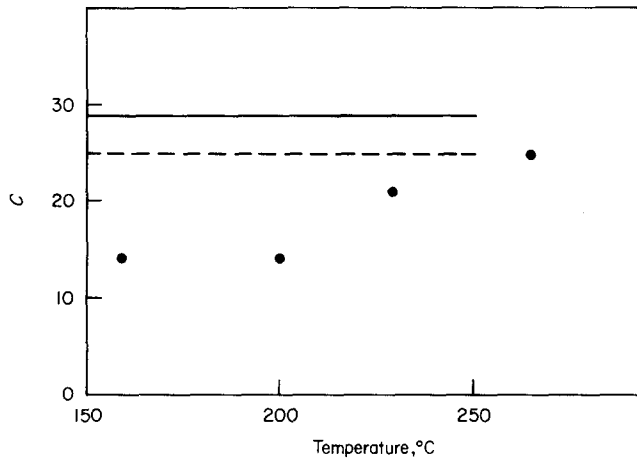


Fig. 11 Coefficient C of the BET equation (see text) as a function of the sintering temperature. The solid line indicates the value of C for the original Japanese 700 Å powder, and the broken line that of the compressed powder

samples treated at high temperatures agrees well with that estimated from the measured particle size of $\sim 0.5 \mu\text{m}$.

The BET results can be understood considering the conclusions of the SEM measurements. The contamination of the surface results in the formation of large clusters of $\sim 0.5 \mu\text{m}$, with the corresponding decrease in surface area; the degassed sinter has a larger C , stronger adsorption potential, and the measured area agrees with that calculated from the observed particle size.

Japanese 400 Å powder. The powder as taken from the bottle (sample J40) has a much smaller surface area, $2.56 \text{ m}^2 \text{ g}^{-1}$, than expected from the nominal particle size. This can be explained by the observed formation of clusters due to surface contamination.

The clusters are proportionally smaller in the 400 Å than in the 700 Å powder. The former would then be 'cleaner', as confirmed by the high value of the C BET coefficient (~ 37) and the fact that this powder adsorbs a substantial amount of gas even at low pressures ~ 3 torr, Fig. 12.

French powder. The surface area of the powder, $\sim 1.3 \text{ m}^2 \text{ g}^{-1}$, agrees roughly with an estimation based on the measured 'particle size' of $\sim 1 \mu\text{m}$, taking into account the large variations in shape and size shown in Fig. 1. A large reduction (50%) of the surface

area is observed even for sintering temperatures as low as 160°C . The values of the C coefficient are low (see Table 1) and the adsorption at low pressures, below 10 torr, is small.

No attempt has been made to sinter the powder at higher temperatures to 'clean' the powder; the specific areas are already too small for their application in heat exchangers.

Furthermore, the equilibrium time for the pressure during the measurement of the isotherms, which is very short with the Japanese powders (tens of seconds) is of the order of 10 min. The porosity of the sinter made out of french powder is very low, reducing its efficiency as heat exchangers.

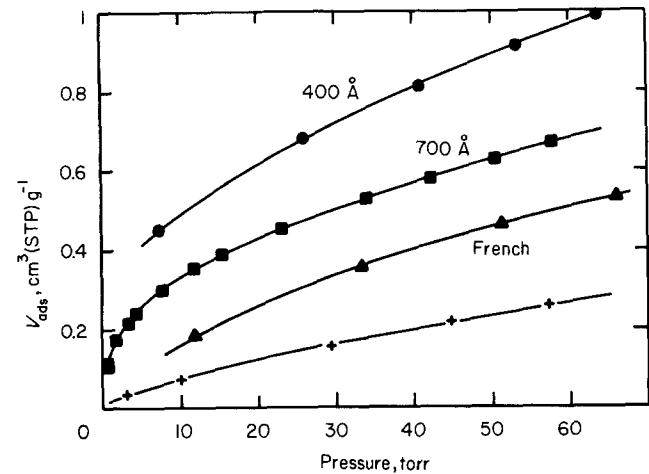


Fig. 12 Argon adsorption isotherm at 77 K of silver powders: volume (STP) of adsorbed argon gas per gram of silver as a function of the equilibrium pressure. ● 400 Å Japanese powder; ■ 700 Å Japanese powder; ▲ French powder; + French powder sintered at 160°C

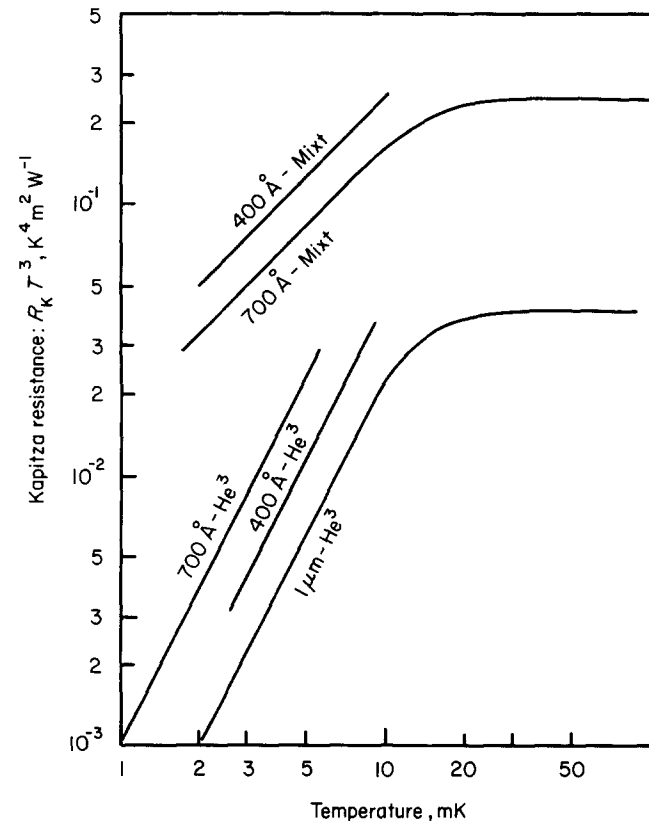


Fig. 13 Typical values of the Kapitza resistance between sintered silver powders and He^3 or He^3/He^4 mixtures, plotted as $R_K T^3$ vs T

Kapitza resistance at ultralow temperatures

The temperature difference between the two media is $\Delta T = R_K \dot{Q}/A$ where \dot{Q} is the heat flux across the interface, A the surface area, and R_K the Kapitza resistivity,^{2,3} which increases at low temperatures as T^{-p} ($p \geq 1$). Sintered metallic powders have been used to achieve thermal contact between a metal and helium.¹ The design of low temperature heat exchangers requires a quantitative knowledge of the Kapitza resistance per unit area R_K . We give in this section typical values of R_K for sintered silver powders, (Fig. 13) obtained by the standard technique, measuring ΔT as a function of \dot{Q} , or by the thermodynamical analysis of the operation of dilution refrigerators, in the case of mixtures. A sinter thickness of the order of 1 mm was used to reduce the temperature gradients.¹⁰

Pure liquid He³. Below 10 mK R_K is proportional to T^{-1} .

400 Å silver powder: $2.6 \text{ mK} < T < 10 \text{ mK}$, $R_K = 470 \text{ T}^{-1} \text{ K}^2 \text{ m}^2 \text{ W}^{-1}$. In a second experimental set up the value $R_K = 900 \text{ T}^{-1} \text{ K}^2 \text{ m}^2 \text{ W}^{-1}$ was found.

700 Å silver powder: $T < 10 \text{ mK}$; $R_K = 1000 \text{ T}^{-1} \text{ K}^2 \text{ m}^2 \text{ W}^{-1}$. In good agreement with the results of Ahonen *et al.*,¹⁹ $R_K = 1100 \text{ T}^{-1} \text{ K}^2 \text{ m}^2 \text{ W}^{-1}$. The Kapitza resistance per unit volume is then $R_K TV = 130 \cdot 10^{-6}$ (MKS), to be compared with the value of $\sim 60 \cdot 10^{-6}$ (MKS), found by Berg and Ihas²⁰ for 700 Å compressed powder.

1 μm silver powder, Andres and Sprenger²¹ give the following results, $1.5 \text{ mK} < T < 10 \text{ mK}$, $R_K \sim 250 \text{ T}^{-1} \text{ K}^2 \text{ m}^2 \text{ W}^{-1}$.

He³-He⁴ mixtures. Below 10 mK: in the case of mixtures, the surfaces are covered by one to two (depending on the nature and the state of the surface) solid layers of pure He⁴, even if the He⁴ is later added to pure He³ at low temperatures.²²

With a coverage of 2 He⁴ layers the measured Kapitza resistance is the same as that found with dilute solutions. Therefore, R_K does not depend on the concentration of He⁴, if the amount of He⁴ in the mixture is large enough to form ~ 2 layers on all the surfaces of the experimental cell.

Such R_K values, typical of 'mixtures', will be found even for 'pure He³' in cells of small surface area ($\sim 100 \text{ cm}^2$), since a He⁴ concentration of several ppm will be enough to form a few atomic layers of He⁴ on the surfaces, with a typical areal density of 10^{19} atoms m^{-2} .

R_K is found to be proportional to T^{-2} below 10 mK for dilute mixtures.

400 Å silver powder: $2 \text{ mK} < T < 10 \text{ mK}$. Different experiments gave the values $R_K = 35 \text{ T}^{-2} \text{ K}^3 \text{ m}^2 \text{ W}^{-1}$,²³ and $R_K = 25 \text{ T}^{-2} \text{ K}^3 \text{ m}^2 \text{ W}^{-1}$.

Heat exchangers for dilution refrigerators built with this powder gave worse results than identical ones made with 700 Å powder.

700 Å silver powder: $2 \text{ mK} < T < 10 \text{ mK}$: the analysis of the performance of dilution refrigerators at $T < 10 \text{ mK}$ gives $R_K = 14 \text{ T}^{-2} \text{ K}^3 \text{ m}^2 \text{ W}^{-1}$.⁷ Osheroff and Corruccini²⁴ also found that R_K is proportional to T^{-2} in mixtures: for 700 Å particles, $0.8 \text{ mK} < T < 4 \text{ mK}$, $R_K = 16.2 \text{ T}^{-2} \text{ K}^3 \text{ m}^2 \text{ W}^{-1}$.

For mixtures ($10 \text{ mK} < T < 100 \text{ mK}$): R_K is approximately proportional to T^{-3} in this temperature range.

700 Å silver powder: From the analysis of the performance of dilution refrigerators⁷: $R_K = 0.24 \text{ T}^{-3} \text{ K}^4 \text{ m}^2 \text{ W}^{-1}$.

Conclusions

The French powder gives a sintered material with a small porosity, and should not be used for heat exchangers below 10 mK. As it sticks better than the Japanese powder on metallic surfaces (as expected from the observed particle's shape), a thin layer of French powder is usually intercalated between the metal and the Japanese powder.⁷

The Japanese 700 Å powder provides large surface areas even after sintering (1 to $2 \text{ m}^2 \text{ g}^{-1}$ depending on the batch used), a good porosity, and a relatively low Kapitza resistance. The specific area of the 400 Å Japanese powder is larger ($\sim 2.6 \text{ m}^2 \text{ g}^{-1}$). Its Kapitza resistance with pure He³ is rather smaller than that of the 700 Å powder. This powder is therefore suitable for cooling pure liquid He³.

On the other hand, it does not seem to be useful for mixtures, since the larger Kapitza resistance is not even compensated by the increase in specific area; the 700 Å powder should be used in this case. The enhancement of the Kapitza resistance in the finer powders is probably due to the exclusion of the He³ from the sinter.

The origin of the surface contamination of the Japanese powder is not yet understood. The weight fraction of the contaminant is small, of the order of 0.005. Nevertheless, this corresponds to many atomic layers covering the surface, and could affect the heat transfer properties. The vicinity of the degassing and sintering temperatures makes this problem difficult to overcome.

On the other hand, the low sintering temperature, combined with the large specific area and good thermal properties, makes the use of the 'spherical' Japanese powders very practical and efficient for low temperature research. The appropriate sintering conditions are obtained with 200°C during 45 min, in agreement with previous results.⁷

Authors

The authors are from the Centre des Recherches sur les Très Basses Températures, (CRTBT-CNRS) BP 166X, 38042 Grenoble-Cédex, France. HF has a fellowship grant from CNPq, Brazil and JB has a fellowship grant from DGRST, France. Paper received April 1984.

The authors acknowledge M. Dupuy and P. Carrier for their help with the SEM measurements at the LETI (Laboratoire d'Electronique et de Technologie de l'Informatique, CEN-Grenoble, CEA).

References

- 1 Lounasmaa, O.V. Experimental principles and methods below 1 K. Academic Press, NY (1974)
- 2 Pollack, G.L. *Rev Mod Phys* **41** (1969) 48
- 3 Harrison, J.P. *J Low Temp Phys* **37** (1979) 467
- 4 Wheatley, J.D., Vilches, O.E., Abel, W.R. *Physics* **4** (1968) 1
- 5 Radebaugh, R., Siegarth, J.D., Holste, J.C., Proc Fifth Int Cryogenic Engineering Conf, Kyoto (1974)
- 6 Frossati, G., Thoulouze, D. Proc Sixth Int Cryogenic Engineering Conf, Grenoble (1976)
- 7 Frossati, G., Godfrin, H., Hébral, B., Schumacher, G., Thoulouze, D. Proc ULT Hakoné Symposium, Japan (1977)
- 8 Frossati, G. *J Phys (Paris)* **39** (1978) C6-1578
- 9 Beal-Monod, M.T., Mills, D.L. *J Low Temp Phys* **30** (1978) 289
- 9 Guillon, F., Harrison, J.P., McMullen, J.T.C., Tyler, A. *Phys Rev Lett* **47** (1981) 435

- 10 **Krusius, M., Paulson, D.N., Wheatley, J.C.** *Cryogenics*, **18** 12 (1978) 649
- 11 **Robertson, R.J., Guillon, F., Harrison, J.P.** *Can J Phys* **61** (1983) 164
- 12 Paillettes d'argent XRP5 Comptoir Lyon Alemand-Louyot, 13 rue de Montmorency 75139 Paris, France
- 13 Ultrafine silver powder (400 Å or 700 Å). Ulvac Metallurgical Co. Ltd., Shonan Bldg 14-10, 1-Chome, Chuo-ku, Tokyo, Japan
- 14 **Brunauer, S., Emmett, P.H., Teller, E.**, *J Am Chem Soc* **60** (1938) 309
- 15 The solid-gas interface, ed. E.A. Flood, Marcel Dekker Inc., New York (1967)
- 16 Micromeritics 2100E Analyser manual, recommended specific areas; Coultronics, 14 rue Eugène Legendre, Margency 95580, Andilly, France
- 17 **Daunt, J.G., Lerner, E. J.** *Low Temp Phys* **8** (1972) 79
- 18 **K. Neumaier** private communication
- 19 **Ahonen, A.I., Lounasmaa, O.V., Veuro, M.C.**, *J Phys (Paris)* **39** (1978) C6-265
- 20 **Berg, R.F., Ihas, G.G.** AIP Conference Proceedings Symposium on Quantum Fluids and Solids, Sanibel Island, Florida, April 11-15 (1983) Ed. Adams, E.D. and Ihas, G.G., AIP (1983)
- 21 **Andres, K., Sprenger, W.O.** Proc 14th Int Conf Low Temp Phys, Ottaniemi, Finland (1975)
- 22 **Godfrin H., Frossati, G., Thoulouze, D., Chapellier, M., Clark, W.G.** *J Phys (Paris)* **39** (1978) C6-287
- 23 **Godfrin, H., Frossati, G., Hébral, B., Thoulouze, D.** *J Phys (Paris)* **41** (1980) C7-275
- 24 **Osheroff, D.D., Corruccini, L.R.** *Phys Lett* **82A** (1981) 38